



# Geophysical Research Letters

## RESEARCH LETTER

10.1029/2019GL086050

### Key Points:

- Eddy-induced surface heat flux anomalies act to dissipate the eddy potential energy
- Enhanced dissipation of eddy potential energy reduces its conversion to eddy kinetic energy, weakening the eddy restratification flux
- The reduced eddy restratification flux weakens the thermal stratification in the upper ocean and results in sea surface cooling

### Supporting Information:

- Supporting Information S1
- Data Set S1

### Correspondence to:

Z. Jing,  
jingzhao198763@sina.com

### Citation:

Shan, X., Jing, Z., Gan, B., Wu, L., Chang, P., Ma, X., et al. (2020). Surface heat flux induced by mesoscale eddies cools the Kuroshio-Oyashio extension region. *Geophysical Research Letters*, 47, e2019GL086050. <https://doi.org/10.1029/2019GL086050>

Received 30 OCT 2019

Accepted 23 DEC 2019

Accepted article online 3 JAN 2020

## Surface Heat Flux Induced by Mesoscale Eddies Cools the Kuroshio-Oyashio Extension Region

Xuan Shan<sup>1</sup>, Zhao Jing<sup>1</sup>, Bolan Gan<sup>1</sup>, Lixin Wu<sup>1</sup>, Ping Chang<sup>1,2,3</sup>, Xiaohui Ma<sup>1</sup>, Shengpeng Wang<sup>1</sup>, Xiaohui Chen<sup>1</sup>, and Haiyuan Yang<sup>1</sup>

<sup>1</sup>Key Laboratory of Physical Oceanography/Institute for Advanced Ocean Studies, Ocean University of China and Qingdao National Laboratory for Marine Science and Technology, Qingdao, China, <sup>2</sup>Department of Oceanography, Texas A&M University, College Station, TX, USA, <sup>3</sup>Department of Atmospheric Sciences, Texas A&M University, College Station, TX, USA

**Abstract** Sea surface temperature (SST) is a key player in the air-sea interaction, influencing storm tracks, atmospheric circulation, and climate modes. Although prevailing theories attribute variations of large-scale SST to atmosphere forcing and ocean internal dynamics, we find that sea surface heat flux anomalies induced by mesoscale eddies exert significant influences on the upper-ocean heat budget in the Kuroshio-Oyashio extension region. Despite making nearly no contribution to the net heat exchange at the air-sea interface, the eddy-induced heat flux anomalies weaken the thermal stratification in the upper ocean and result in pronounced sea surface cooling. The underlying dynamics is the efficient dissipation of eddy potential energy by eddy-induced heat flux anomalies. This makes the conversion of eddy potential energy to eddy kinetic energy significantly reduced, corresponding to a weaker eddy-induced restratification flux. The finding complements the existing theories on large-scale SST dynamics and has important implications for understanding extratropical climate variability.

**Plain Language Summary** Sea surface temperature (SST) plays a fundamental role in the air-sea interactions. At large scales (~1,000 km), it is traditionally thought that the atmospheric forcing drives the midlatitude SST variability. At mesoscales (~100 km), it is an ocean-driven scenario where pronounced SST anomalies carried by ocean eddies exert an imprint on the atmospheric boundary layer. In this study, we find that such ocean mesoscale-atmosphere (OME-A) interactions have a significant influence on the large-scale SST in the Kuroshio-Oyashio extension region, complementing the existing views on the large-scale SST dynamics. This is because the eddy-induced heat flux anomalies damp the SST anomalies and thus available potential energy of eddies. Correspondingly, the conversion of eddy available potential energy to kinetic energy is significantly reduced in presence of OME-A interactions, resulting in less heat transported from the subsurface to the surface region.

## 1. Introduction

The ocean and atmosphere are a highly coupled system with the sea surface temperature (SST) playing a fundamental role in their coupling (Kushnir et al., 2002; Kwon et al., 2010). Dynamics of SST in the extratropical region have been extensively studied in the past few decades. In the canonical theories, variations of extratropical SST at large scales (~1,000 km) are primarily explained by atmospheric forcing and basin-scale oceanic processes (Alexander, 2010; Frankignoul, 1985; Kwon et al., 2010). On seasonal and shorter time scales, large-scale SST anomalies (SSTAs) are modulated by changes in the air-sea heat flux (Frankignoul & Kestenare, 2002), especially in winter when cold and dry air outbreaks move from continents to the warmer sea surface (Xue et al., 1995). On longer time scales, the contribution of heat advection due to geostrophic and Ekman currents becomes important (Dong & Kelly, 2004; Nakamura et al., 1997; Qiu, 2000). In addition, due to the seasonal evolution of mixed layer depth and entrainment, SSTAs form in one winter can reemerge in the following winter (Alexander & Deser, 1995). This reemergence can be nonlocal in the presence of strong advection (Sugimoto & Hanawa, 2005).

Recent studies also reveal the essential role of oceanic eddies in the large-scale SST budget in the extratropical region (Nurser & Zhang, 2000; Su et al., 2018). Eddies produce a significant upward heat transport peaking in the subsurface region associated with the conversion of eddy potential energy (EPE) to eddy kinetic

energy (EKE) (Nurser & Zhang, 2000; von Storch et al., 2012). This vertical eddy heat transport restratifies the upper ocean and increases the SST, similar to the scenario in the atmosphere where baroclinic eddies stabilize the lower part of troposphere and increase the near-ground air temperature (Gutowski, 1985). In the prevailing theories, the intensity of vertical eddy heat transport is explained by ocean internal dynamics such as baroclinic instability and frontogenesis (Eady, 1949; McWilliams, 2016).

High-resolution satellite measurements and eddy-resolving coupled ocean-atmosphere model simulations indicate that eddies at mesoscales (100–1,000 km) interact strongly with the overlying atmosphere (Chelton et al., 2004; Frenger et al., 2013; Small et al., 2008), exerting a significant imprint on the local surface turbulent heat flux, atmospheric boundary layer height, wind/wind stress, and rainfalls. Such ocean mesoscale eddy-atmosphere (OME-A) interactions can further feed back onto eddies through their influences on surface wind stress or heat flux in a variety of ways. The eddy current's imprint on wind stress acts to dissipate EKE (Eden & Dietze, 2009; Renault et al., 2016), while the SSTAs carried by eddies induce a dipolar wind stress curl anomaly, affecting eddies' propagation through Ekman pumping (Gaube et al., 2015; Seo et al., 2016). More recently, the turbulent heat flux anomalies induced by eddies are found to damp mesoscale SSTAs (Bishop et al., 2017; Li et al., 2017), leading to a destruction of EPE (Ma et al., 2016; Yang et al., 2018) (referred to as the OME-A EPE feedback henceforth). A particular question this study attempts to address is as follows: Can this OME-A EPE feedback affect the large-scale SST by regulating the vertical eddy heat transport through its impact on the EPE budget?

The manuscript is organized as follows. In section 2, methodology and data are introduced. In section 3, OME-A EPE feedback's effect on the large-scale SST and upper ocean thermal stratification in the Kuroshio-Oyashio extension (KOE) region is presented. Conclusions and discussion are shown in section 4.

## 2. Materials and Methods

### 2.1. Experimental Design

The twin simulations (CTRL and FILT) in the North Pacific are devised using the Coupled Regional Climate Model (CRCM) developed at Texas A&M University (Ma et al., 2016). CRCM includes the Weather Research and Forecasting (WRF) Model as the atmospheric component and the Regional Ocean Modeling Systems (ROMS) as the oceanic component, both having the horizontal resolution of 9 km. The ocean model provides SST and surface current velocity to the atmosphere model and receives updated heat and freshwater fluxes as well as wind stress from the atmosphere model hourly. The heat, freshwater fluxes, and wind stress are computed based on the bulk formula with the ocean surface current's impact on the wind stress included (Large & Yeager, 2009).

Both CTRL and FILT simulations consist of an ensemble of five 6-month integrations, initialized on the 1st of October 2003, 2004, 2005, 2006, and 2007. For each ensemble pair, CTRL and FILT share the same initial conditions. The WRF initial condition is obtained from NCEP-II reanalysis, whereas the ROMS initial condition is obtained from a 6-year spin-up run using CORE-II data set as the atmospheric forcing. The 6-month integration is short enough to rule out the remote influences through planetary waves (Qiu & Chen, 2005), isolating the SST change due to the local OME-A EPE feedback. Moreover, as demonstrated in section 3, it is still long enough to allow the response of EPE and SST to the OME-A EPE feedback to reach a roughly stable state. The winter season is chosen, because the OME-A interaction is strong during that time.

The FILT ensemble is conducted with the same settings as the CTRL except that a low-pass Loess filter with  $15^\circ$  (longitude)  $\times 5^\circ$  (latitude) half width (the cutoff wavelength is  $16^\circ$  in zonal direction and  $6^\circ$  in meridional direction) is applied to the ROMS simulated SST before being provided to WRF at each coupling step (No filter is performed on ocean surface currents), making the atmosphere unable to "feel" the mesoscale SST variability. Therefore, the OME-A EPE feedback is largely suppressed in FILT and the difference between CTRL and FILT allows us to evaluate the impact of OME-A EPE feedback on the large-scale SST. More details on the configuration of CRCM can be found in Ma et al. (2016).

### 2.2. Heat Budget Analysis

To discuss the thermal condition of the upper ocean, we perform the heat budget analysis:

$$\rho_0 C_p \left\langle \frac{\partial T}{\partial t} \right\rangle = -\rho_0 C_p \left\langle \nabla \cdot (\bar{\mathbf{u}} \bar{T}) \right\rangle - \rho_0 C_p \left\langle \nabla_{\mathbf{h}} \cdot (\mathbf{u}' \bar{T}') \right\rangle - \rho_0 C_p \left\langle \frac{\partial w' T'}{\partial z} \right\rangle - \left\langle \frac{\partial Q}{\partial z} \right\rangle, \\ -\rho_0 C_p \left\langle \nabla \cdot (\bar{\mathbf{u}} \bar{T}') + \nabla \cdot (\mathbf{u}' \bar{T}) \right\rangle \quad (1)$$

where  $\langle \dots \rangle$  denotes an area average in the KOE region ( $36\text{--}44^\circ\text{N}$ ,  $147.5\text{--}162^\circ\text{E}$ ) plus a time average over the last 90-day model integration,  $T$  is the temperature,  $\mathbf{u} = (u, v, w)$  is the three-dimensional velocity,  $\mathbf{u}_{\mathbf{h}} = (u, v)$  is the horizontal velocity,  $w$  is the vertical velocity,  $\nabla = (\partial/\partial x, \partial/\partial y, \partial/\partial z)$ ,  $\nabla_{\mathbf{h}} = (\partial/\partial x, \partial/\partial y)$ ,  $\rho_0 = 1,025 \text{ kg m}^{-3}$  is the ocean reference density,  $C_p = 4,000 \text{ J kg}^{-1} \text{ }^\circ\text{C}^{-1}$  is the ocean heat capacity approximated as a constant here,  $Q$  is the vertical turbulent heat transport defined positive upward.

Variables in equation (1) denoted by primes and bars correspond to the mesoscale eddies and large-scale background flows, respectively. In this study, the mesoscale anomalies are isolated from the large-scale background motions by spatial filtering which is the standard way in the existing studies on OME-A interactions (e.g., Chelton et al., 2004; O'Neill et al., 2010; Perlin et al., 2014; Seo et al., 2016). A 2-D Gaussian filter is used with its standard deviation parameter tuned to mimic the performance of the  $15^\circ$  (longitude)  $\times 5^\circ$  (latitude) Loess filter to keep consistency. As displayed in supporting information Figure S1, the mesoscale variabilities in the spatial and spectral spaces obtained from these two filters are almost identical. But using the Gaussian filter leads to a substantial reduction of the computational burden.

The term on the left-hand side of equation (1) is the change rate of heat, which is balanced by terms on the right-hand side of equation (1). The terms on the right-hand side in sequence are the heat advection by large-scale background flows, the horizontal eddy heat transport convergence, the vertical eddy heat transport convergence, the vertical turbulent heat transport convergence (referred to as the vertical mixing), and the residue term. The residue term does not have a clear dynamical interpretation but would be zero if the large-scale motions are obtained using a time or zonal mean as in the classical eddy-mean flow interaction theories rather than the spatial filter we use. Because it has no counterpart in the classical eddy-mean flow interaction theories, it is referred to as the residue term. The residue term is found to be an order of magnitude smaller than the other terms and can be neglected. The horizontal mixing is dropped in equation (1) as the horizontal diffusivity is set as zero in CRCM simulations.

### 2.3. Mesoscale Temperature Anomaly Variance Budget

In order to evaluate the OME-A EPE feedback's impact on the eddy energy budget, the mesoscale temperature anomaly variance budget (see Text S2 for the detailed derivation) regarded as a proxy for EPE budget is performed:

$$\left\langle \frac{\partial}{\partial t} \left( \frac{1}{2} T'^2 \right) \right\rangle = -\left\langle \nabla \cdot \left( \frac{1}{2} \mathbf{u} T'^2 \right) \right\rangle - \left\langle \mathbf{u}' \bar{T}' \cdot \nabla_{\mathbf{h}} \bar{T} \right\rangle - \left\langle w' T' \frac{\partial \bar{T}}{\partial z} \right\rangle - \left\langle T' \frac{\partial}{\partial z} \left( \frac{Q'}{\rho_0 C_p} \right) \right\rangle, \\ -\left\langle \bar{\mathbf{u}} T' \cdot \nabla \bar{T} \right\rangle + \left\langle T' \bar{\mathbf{u}} \cdot \nabla \bar{T} \right\rangle \quad (2)$$

The term on the left-hand side of equation (2) is the tendency of mesoscale temperature anomaly variance determined by the production and destruction processes on the right-hand side. The first term on the right-hand side is the advection of mesoscale temperature anomaly variance. The second term is the horizontal eddy temperature transport acting on the temperature gradient of mean flows. It denotes the energy conversion from available potential energy of mean flows (MPE) to EPE (von Storch et al., 2012), referred to as the MPE-EPE conversion. The third term is the vertical eddy temperature transport acting on the background thermal stratification associated with the conversion of EPE to EKE (referred to as the EPE-EKE conversion). The fourth term is the dissipation through vertical mixing (referred to as the vertical dissipation). The last two terms have no clear dynamical meanings and referred to as the residue term. Again, the dissipation through horizontal mixing is dropped here as the horizontal diffusivity is set as zero in CRCM simulations. The OME-A EPE feedback contributes to the budget through the vertical dissipation term as evidenced by its decomposition into the surface term and the interior dissipation term:

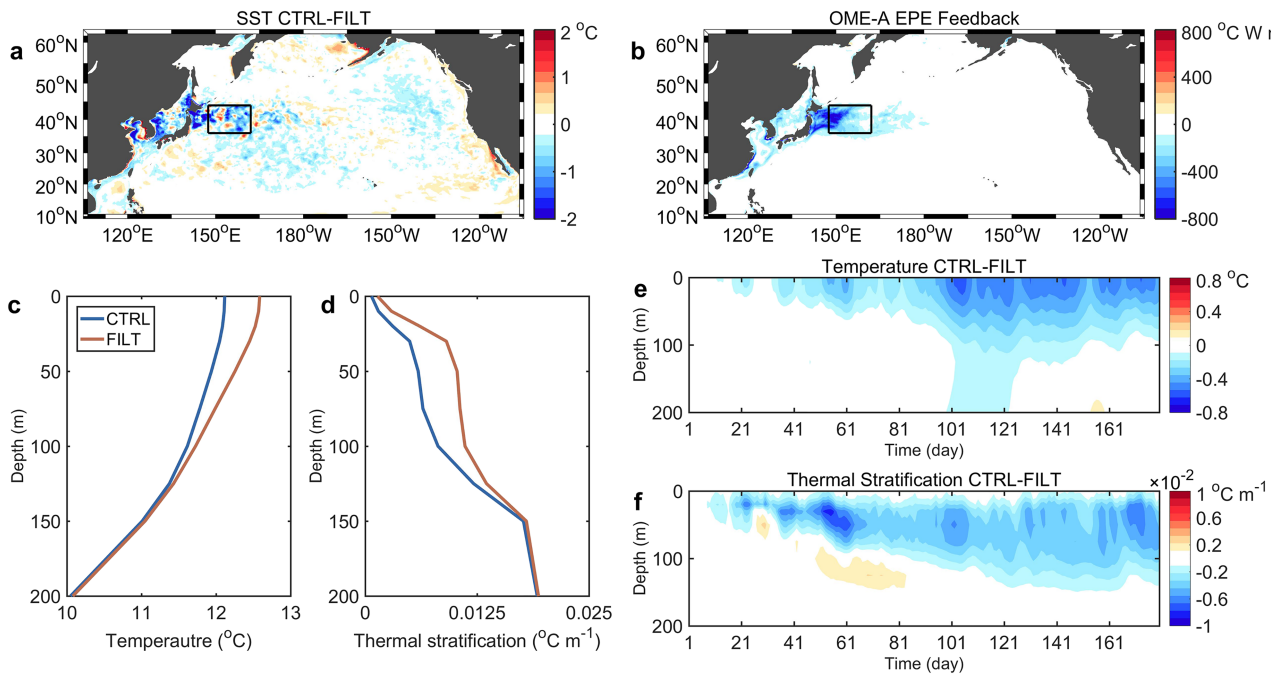


**Figure 1.** SST difference in CTRL and FILT simulations. (a) Time-mean SST in CTRL minus that in FILT; (b) time-mean OME-A EPE feedback measured by  $-T'Q|_{z=0}$  ( $Q$  is defined positive upward) in CTRL; time-mean (c) temperature profiles and (d) thermal stratification profiles in CTRL and FILT in the KOE region (denoted by the black boxes in (a) and (b),  $36\text{--}44^{\circ}\text{N}$ ,  $147.5\text{--}162^{\circ}\text{E}$ ); time series of (e) temperature and (f) thermal stratification in CTRL minus those in FILT. All values shown here are the ensemble mean and only the values in the last 90-day model integration are used for the computation of time mean.

$$-\langle \int_{z_b}^0 T' \frac{\partial}{\partial z} \left( \frac{Q'}{\rho_0 C_p} \right) dz \rangle = -\frac{\langle T' Q' |_{z=0} \rangle}{\rho_0 C_p} + \underbrace{\frac{\langle T' Q' |_{z=z_b} \rangle}{\rho_0 C_p}}_{\text{interior dissipation}} + \langle \int_{z_b}^0 \frac{\partial T'}{\partial z} \cdot \frac{Q'}{\rho_0 C_p} dz \rangle. \quad (3)$$

The surface term ( $-T'Q'|_{z=0}$ ), representing the OME-A EPE feedback, is negative in CTRL as a result of eddy-induced heat flux anomalies (Figure 1b) but is much reduced in FILT (Figure S2).

#### 2.4. Statistical Analysis

The error bar of the ensemble mean difference (CTRL-FILT) in this study is defined as  $[X - 3\sigma_e, X + 3\sigma_e]$  with  $X$  the sample mean difference and  $\sigma_e$  its standard error:

$$X = \frac{1}{n} \sum_{j=1}^n x_j, \quad (4)$$

$$\sigma_e = \sqrt{\frac{\sum_{j=1}^n (x_j - X)^2}{n-1}} / \sqrt{n}, n = 5, \quad (5)$$

where  $x_j$  is the difference between CTRL and FILT of the  $j$ th ensemble member.

### 3. Results

#### 3.1. Difference of SST Between CTRL and FILT

Figure 1a shows the ensemble mean SST difference between CTRL and FILT averaged for the last 90 days of the simulations when the SST difference seems to become roughly stable (Figure 1e). There is a systematic sea surface cooling in CTRL compared to FILT. The SST difference between CTRL and FILT is generally less than  $0.5^{\circ}\text{C}$  in the North Pacific basin except in the KOE region where the value can reach up to  $2^{\circ}\text{C}$  locally. In the KOE region, the relative cooling in CTRL is most evident in the upper 50 m and the signal attenuates rapidly as the depth increases (Figure 1c). Such surface-intensified cooling in CTRL corresponds to a

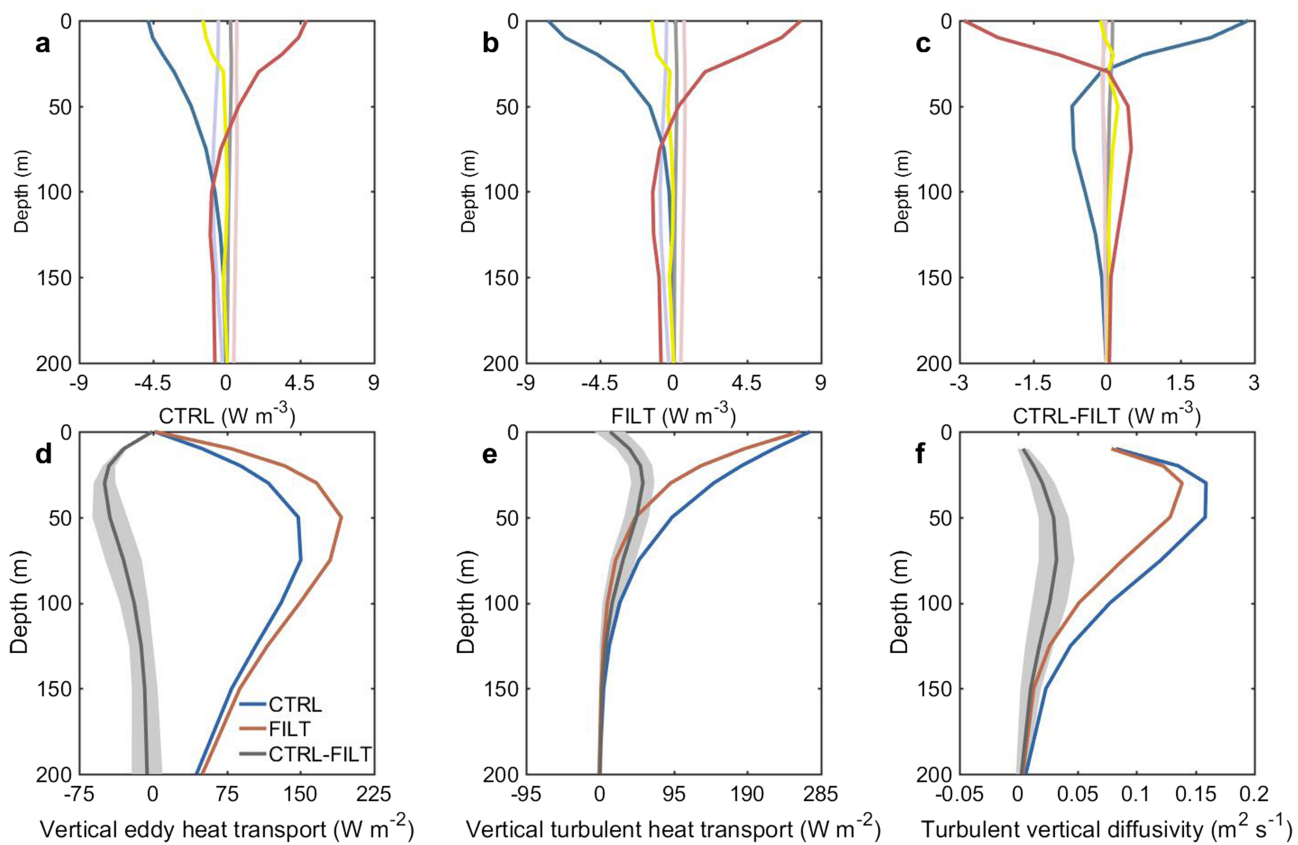


**Figure 2.** Heat budget in the KOE region. The heat budget averaged over the KOE region in (a) CTRL, (b) FILT, and (c) CTRL-FILT. The red line denotes the vertical eddy heat transport convergence. The blue line denotes the vertical mixing. The yellow line denotes the heat advection by large-scale background flows. The pink line denotes the horizontal eddy heat transport convergence. The purple line denotes the change rate of heat. The grey line denotes the residue. Time-mean (d) vertical eddy heat transport, (e) vertical turbulent heat transport, and (f) turbulent vertical diffusivity in CTRL (denoted by blue lines) and FILT (denoted by red lines) in the KOE region. Note that the ROMS does not output the turbulent vertical diffusivity at the sea surface (Haidvogel et al., 2008). The grey shading indicates the error bar with detailed descriptions in section 2. All values shown here are the ensemble mean and only the values in the last 90-day model integration are used for the computation of time mean.

weakened thermal stratification measured by the vertical temperature gradient. Indeed, the thermal stratification in the upper 100 m is systematically weaker in CTRL than in FILT with its vertical mean value in CTRL only 60% of that in FILT (Figures 1d and 1f). The largest temperature difference in the KOE region coincides well with the strongest OME-A EPE feedback (Figure 1b). Such coincidence implies that the surface cooling in CTRL might result from the OME-A EPE feedback.

To test this hypothesis, a heat budget analysis for the KOE region is performed based on the last 90-day diagnostic output from CRCM. In both CTRL and FILT, there is a dominant balance in the upper ocean between the cooling caused by the vertical mixing and the warming by the vertical eddy heat transport convergence (Figures 2a and 2b), with the remaining terms playing a minor role. The former is a result of strong surface heat release from the ocean to the atmosphere in the winter time, while the latter is due to the upward eddy heat transport associated with the conversion of EPE to EKE (Figure 2d). This vertical eddy heat transport, peaking around 50 m, acts to restratify the upper ocean and plays a crucial role in resisting the surface cooling caused by the heat release in the upper ocean.

It is evident from the heat budget difference between CTRL and FILT that the reduced thermal stratification and decreased SST in the KOE region in CTRL are primarily attributed to the change of the vertical eddy heat transport convergence which causes more cooling near the sea surface (Figure 2c). In presence of the OME-A EPE feedback, the vertical eddy heat transport is significantly weakened, with a maximum reduction of  $49 \pm 11 \text{ W m}^{-2}$  around 30 m (Figure 2d). Their difference (CTRL-FILT) corresponds to a

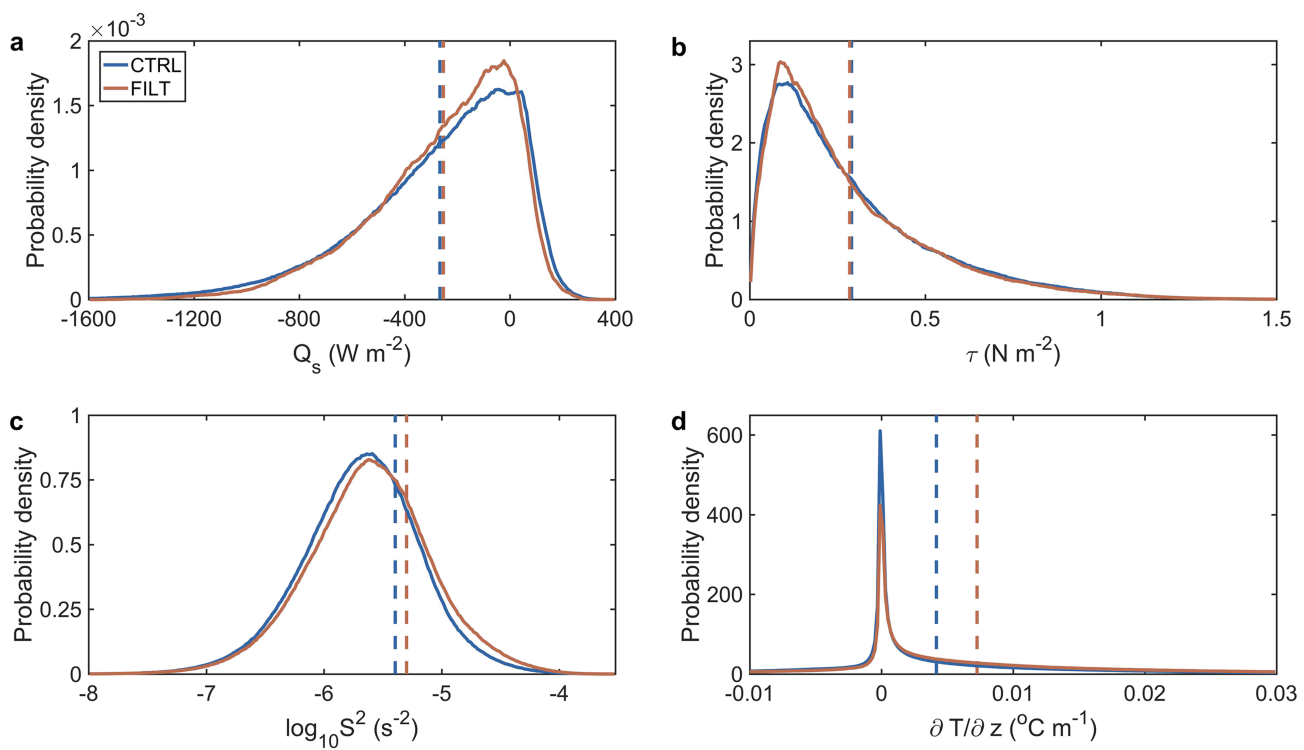


**Figure 3.** Factors controlling the intensity of small-scale turbulence. The probability density function of (a) sea surface heat flux, (b) wind stress magnitude, (c) vertical shear variance, and (d) thermal stratification in CTRL (denoted by blue lines) and FILT (denoted by red lines) in the KOE region. The dashed lines show the mean values. Only the values in the last 90-day model integration are used.

destratification flux (the opposite of a restratification flux), contributing to the weakened thermal stratification and cooled sea surface in CTRL.

The difference of the vertical eddy heat transport convergence is largely balanced by the difference of the vertical mixing (Figure 2c) so that an equilibrium state of the upper ocean temperature difference between CTRL and FILT can be established. The advection by large-scale flows and the horizontal eddy heat transport convergence play the secondary if not negligible roles with their total contribution less than 25%. Compared to FILT, the vertical mixing in CTRL results in less cooling near the sea surface but more cooling in the deeper region (Figure 2c). The vertical mixing difference between CTRL and FILT is not due to the change of the area-mean heat flux at the air-sea interface but mainly results from the differed decay rate of vertical turbulent heat transport in the ocean. The net heat loss at the sea surface averaged over the KOE region is  $271 \text{ W m}^{-2}$  in CTRL, fairly close to  $258 \text{ W m}^{-2}$  in FILT (Figure 2e). Their difference,  $13 \pm 20 \text{ W m}^{-2}$  is not significantly different from zero, suggesting that the surface heat flux anomalies induced by mesoscale eddies do not directly make significant contribution to the net heat exchange at the air-sea interface. However, the vertical turbulent heat transport decays more slowly with depth in CTRL than in FILT (Figure 2e) as a result of enhanced turbulent vertical diffusivity in CTRL (Figure 2f), making the near-surface (deeper) region less (more) cooled. The difference of the vertical turbulent heat transport results in a restratification flux which largely compensates the destratification flux caused by the difference of the vertical eddy heat transport mentioned above. In the surface ocean boundary layer, the intensity of small-scale turbulence is basically determined by the sea surface buoyancy flux (dominated by heat flux), wind stress magnitude, vertical shear, and stratification (Large et al., 1994). It is found that the larger turbulent vertical diffusivity in CTRL is mainly attributed to the weakened stratification with the first three factors playing a negligible or countering role (Figure 3). Therefore, the change of the vertical mixing is unlikely to be directly caused by the OME-A interaction but is an indirect result of it through its impact on the vertical eddy heat transport and further on the stratification.

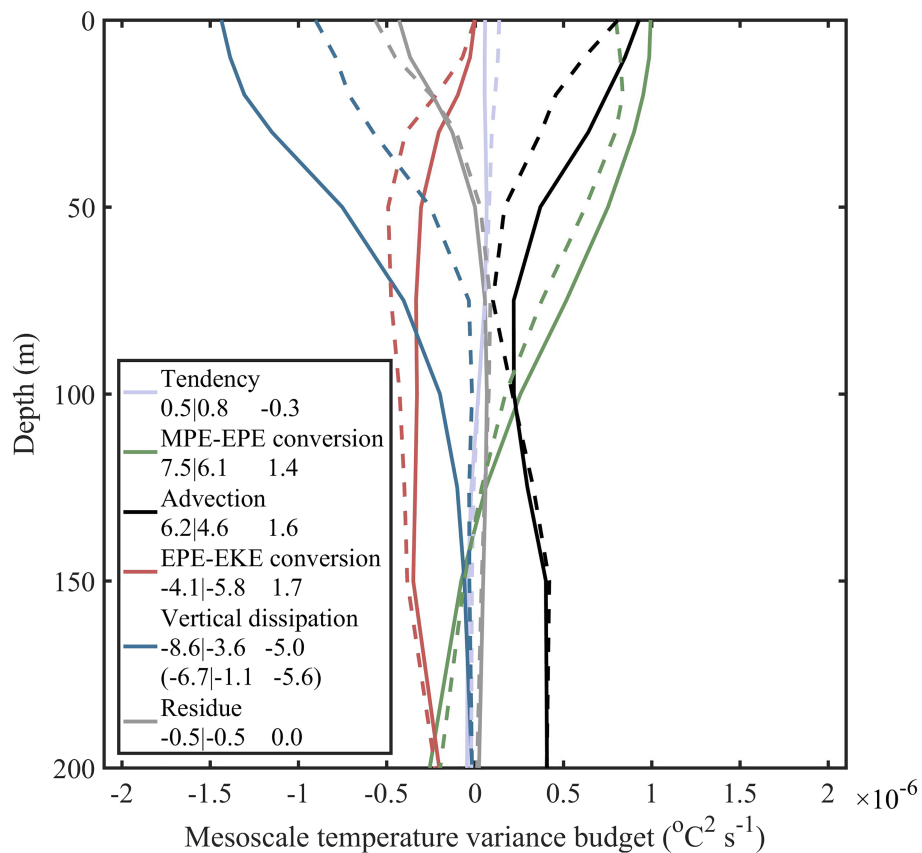


**Figure 4.** Mesoscale temperature variance budget in the KOE region. The solid and dashed lines correspond to the CTRL and FILT, respectively. The table in the left-lower corner shows the values ( $\times 10^{-5} \text{ }^{\circ}\text{C}^2 \text{ m s}^{-1}$ ) integrated in the upper 150 m in CTRL, FILT, and CTRL-FILT. The values in the bracket represent the contribution of OME-A EPE feedback. All values shown here are the ensemble mean averaged over the last 90-day model integration.

### 3.2. Impact of OME-A EPE Feedback on the Vertical Eddy Heat Transport

As demonstrated in section 3.1, the reduction of vertical eddy heat transport leads to the sea surface cooling and weakened thermal stratification in CTRL. In this subsection, we attempt to understand the underlying dynamics responsible for the reduced vertical eddy heat transport. In FILT, the atmosphere is unable to “feel” the mesoscale SSTAs variability so that the OME-A EPE feedback is largely suppressed. Meanwhile, the mesoscale SSTAs imprints on surface wind and their feedback on Ekman pumping (Chelton et al., 2004; Gaube et al., 2015) are also filtered out. We find that the latter related transport variation at the base of the Ekman layer (Thomas & Ferrari, 2008) is unlikely to account for the difference of computed vertical eddy heat transport between CTRL and FILT (see Text S1 and Figure S3 for details, Thomas & Ferrari, 2008). It thus implies that the weakened vertical eddy heat transport in CTRL might be due to the OME-A EPE feedback. To confirm this conjecture, a mesoscale temperature anomaly variance (closely related to the mesoscale EPE) budget over the KOE region during the last 90-day model integration is performed (Figure 4).

In both CTRL and FILT, there is in general a balance between the production and destruction terms of mesoscale temperature anomaly variance on the right-hand side of equation (2), with negligible tendency of mesoscale temperature anomaly variance. The production is achieved primarily through the advection and MPE-EPE conversion, while the destruction results mainly from two processes: the vertical dissipation and EPE-EKE conversion. The OME-A EPE feedback has a profound influence on the mesoscale temperature anomaly variance budget in the upper 150 m. In CTRL, the vertical dissipation averaged in the upper 150 m is more than twice as large as that in FILT. The enhanced vertical dissipation is mainly due to the OME-A EPE feedback with the contribution from the interior dissipation negligible. The advection, MPE-

EPE conversion, and EPE-EKE conversion all respond significantly to the OME-A EPE feedback and work in concert to balance the intensified destruction of mesoscale temperature anomaly variance in CTRL. In particular, the mean EPE-EKE conversion in the upper 150 m is reduced by 29% in CTRL, compensating ~34% of the enhanced dissipation. This leads to a weakened vertical eddy heat transport in CTRL, lending supports to our hypothesis.

#### 4. Conclusions and Discussion

These results from the high-resolution regional climate model experiments reveal the important role of OME-A EPE feedback in shaping the upper ocean thermal stratification, providing a new perspective on the large-scale SST dynamics and complementing the existing theories. Through damping the EPE, the eddy-induced surface heat flux anomalies reduce the EPE-EKE conversion, leading to a weakened eddy restratification flux. The latter weakens the thermal stratification in the upper ocean and results in sea surface cooling.

Although this study focuses on the KOE region, similar impacts of OME-A interaction on SST are expected to hold in other regions with strong mesoscale eddy activities and air-sea interactions. In addition, the results of this study have important implications for modeling biogeochemical processes in the ocean. In the presence of OME-A EPE feedback, small-scale turbulence in the upper ocean is significantly enhanced due to the weakened stratification. This could further affect the light exposure of phytoplankton and supply of nutrients into the euphotic zone, the two key factors controlling the primary production (Levy et al., 2012). Therefore, the OME-A EPE feedback may be important in maintaining the upper-ocean ecosystem that controls the ocean's storage of carbon and regulates the carbon dioxide level in the atmosphere (Ducklow et al., 2001).

#### Conflict of Interests

The authors declare no competing financial interests.

#### Data and Materials Availability

The data, analysis codes, and information about model configuration used in our study are publicly available from Figshare repository (<http://doi.org/10.6084/m9.figshare.11402691>).

#### Acknowledgments

This research is completed through the International Laboratory for High Resolution Earth System Prediction, a collaboration by the Qingdao National Laboratory for Marine Science and Technology Development Center, Texas A&M University, and the National Center for Atmospheric Research. The regional climate model CRCM was developed by Raffaele Montuoro at TAMU under the direction of P.C. The Texas Advanced Computing Center at The University of Texas and the Texas A&M High Performance Research Computing provided the computing resources we needed to perform our CRCM simulations. This research is supported by National Science Foundation of China (41490643, 41490640, 41822601, 41776006), Taishan Scholar Funds (tsqn201909052), Fundamental Research Funds for the Central Universities (201841011, 201812014), and U.S. National Science Foundation grant AGS-1462127.

#### References

- Alexander, M. (2010). Extratropical air-sea interaction, sea surface temperature variability, and the Pacific Decadal Oscillation. In D. Sun & F. Bryan (Eds.), *Climate Dynamics: Why Does Climate Vary?*, Geophysical Monograph Series (Vol. 189, pp. 123–148). Washington, DC: American Geophysical Union. <https://doi.org/10.1029/2008GM000794>
- Alexander, M. A., & Deser, C. (1995). A Mechanism for the recurrence of wintertime midlatitude SST anomalies. *Journal of Physical Oceanography*, 25(1), 122–137. [https://doi.org/10.1175/1520-0485\(1995\)025<0122:AMFTRO>2.0.CO;2](https://doi.org/10.1175/1520-0485(1995)025<0122:AMFTRO>2.0.CO;2)
- Bishop, S. P., Small, R. J., Bryan, F. O., & Tomas, R. A. (2017). Scale dependence of midlatitude air-sea interaction. *Journal of Climate*, 30(20), 8207–8221. <https://doi.org/10.1175/jcli-d-17-0159.1>
- Chelton, D. B., Schlax, M. G., Freilich, M. H., & Milliff, R. F. (2004). Satellite measurements reveal persistent small-scale features in ocean winds. *Science*, 303(5660), 978–983. <https://doi.org/10.1126/science.1091901>
- Dong, S. F., & Kelly, K. A. (2004). Heat budget in the Gulf Stream region: The importance of heat storage and advection. *Journal of Physical Oceanography*, 34(5), 1214–1231. [https://doi.org/10.1175/1520-0485\(2004\)034<1214:HBITGS>2.0.CO;2](https://doi.org/10.1175/1520-0485(2004)034<1214:HBITGS>2.0.CO;2)
- Ducklow, H. W., Steinberg, D. K., & Buesseler, K. O. (2001). Upper ocean carbon export and the biological pump. *Oceanography*, 14(4), 50–58. <https://doi.org/10.5670/oceanog.2001.06>
- Eady, E. T. (1949). Long waves and cyclone Waves. *Tellus*, 1(3), 33–52. <https://doi.org/10.3402/tellusa.v1i3.8507>
- Eden, C., & Dietze, H. (2009). Effects of mesoscale eddy/wind interactions on biological new production and eddy kinetic energy. *Journal of Geophysical Research*, 114, C05023. <https://doi.org/10.1029/2008JC005129>
- Frankignoul, C. (1985). Sea surface temperature anomalies, planetary waves, and air-sea feedback in the middle latitudes. *Reviews of Geophysics*, 23(4), 357–390. <https://doi.org/10.1029/rg023i004p00357>
- Frankignoul, C., & Kestenare, E. (2002). The surface heat flux feedback. Part I: Estimates from observations in the Atlantic and the North Pacific. *Climate Dynamics*, 19(8), 633–647. <https://doi.org/10.1007/s00382-002-0252-x>
- Frenger, I., Gruber, N., Knutti, R., & Munnich, M. (2013). Imprint of Southern Ocean eddies on winds, clouds and rainfall. *Nature Geoscience*, 6(8), 608–612. <https://doi.org/10.1038/NGEO1863>
- Gaube, P., Chelton, D. B., Samelson, R. M., Schlax, M. G., & O'Neill, L. W. (2015). Satellite observations of mesoscale eddy-induced Ekman pumping. *Journal of Physical Oceanography*, 45(1), 104–132. <https://doi.org/10.1175/jpo-d-14-0032.1>
- Gutowski, W. J. (1985). Baroclinic adjustment and midlatitude temperature profiles. *Journal of the Atmospheric Sciences*, 42(16), 1733–1745. [https://doi.org/10.1175/1520-0469\(1985\)042<1733:BAAMTP>2.0.CO;2](https://doi.org/10.1175/1520-0469(1985)042<1733:BAAMTP>2.0.CO;2)
- Haidvogel, D. B., Arango, H., Budgell, W. P., Cornuelle, B. D., Curchitser, E., Di Lorenzo, E., et al. (2008). Ocean forecasting in terrain-following coordinates: Formulation and skill assessment of the Regional Ocean Modeling System. *Journal of Computational Physics*, 227(7), 3595–3624. <https://doi.org/10.1016/j.jcp.2007.06.016>

- Kushnir, Y., Robinson, W. A., Blade, I., Hall, N. M. J., Peng, S., & Sutton, R. (2002). Atmospheric GCM response to extratropical SST anomalies: Synthesis and evaluation. *Journal of Climate*, 15(16), 2233–2256. [https://doi.org/10.1175/1520-0442\(2002\)015<2233:AGRTE>2.0.CO;2](https://doi.org/10.1175/1520-0442(2002)015<2233:AGRTE>2.0.CO;2)
- Kwon, Y. O., Alexander, M. A., Bond, N. A., Frankignoul, C., Nakamura, H., Qiu, B., & Thompson, L. A. (2010). Role of the Gulf Stream and Kuroshio-Oyashio systems in large-scale atmosphere-ocean interaction: A review. *Journal of Climate*, 23(12), 3249–3281. <https://doi.org/10.1175/2010jcli3343.1>
- Large, W. G., Mcwilliams, J. C., & Doney, S. C. (1994). Oceanic vertical mixing: A review and a model with a nonlocal boundary-layer parameterization. *Reviews of Geophysics*, 32(4), 363–403. <https://doi.org/10.1029/94rg01872>
- Large, W. G., & Yeager, S. G. (2009). The global climatology of an interannually varying air-sea flux data set. *Climate Dynamics*, 33(2-3), 341–364. <https://doi.org/10.1007/s00382-008-0441-3>
- Levy, M., Ferrari, R., Franks, P. J. S., Martin, A. P., & Riviere, P. (2012). Bringing physics to life at the submesoscale. *Geophysical Research Letters*, 39, L14602. <https://doi.org/10.1029/2012GL052756>
- Li, F. R., Sang, H. Y., & Jing, Z. (2017). Quantify the continuous dependence of SST-turbulent heat flux relationship on spatial scales. *Geophysical Research Letters*, 44(12), 6326–6333. <https://doi.org/10.1002/2017GL073695>
- Ma, X. H., Jing, Z., Chang, P., Liu, X., Montuoro, R., Small, R. J., et al. (2016). Western boundary currents regulated by interaction between ocean eddies and the atmosphere. *Nature*, 535(7613), 533–537. <https://doi.org/10.1038/nature18640>
- McWilliams, J. C. (2016). Submesoscale currents in the ocean. *Proceedings of the Royal Society A: Mathematical, Physical and Engineering Sciences*, 472(2189), 20160117. <https://doi.org/10.1098/rspa.2016.0117>
- Nakamura, H., Lin, G., & Yamagata, T. (1997). Decadal climate variability in the North Pacific during the recent decades. *Bulletin of the American Meteorological Society*, 78(10), 2215–2225. [https://doi.org/10.1175/1520-0477\(1997\)078<2215:DCVN>2.0.CO;2](https://doi.org/10.1175/1520-0477(1997)078<2215:DCVN>2.0.CO;2)
- Nurser, A. J. G., & Zhang, J. W. (2000). Eddy-induced mixed layer shallowing and mixed layer/thermocline exchange. *Journal of Geophysical Research, Oceans*, 105(C9), 21,851–21,868. <https://doi.org/10.1029/2000jc000018>
- O'Neill, L., Esbensen, S. K., Thum, N., Samelson, R. M., & Chelton, D. B. (2010). Dynamical analysis of the boundary layer and surface wind responses to mesoscale SST perturbations. *Journal of Climate*, 23(3), 559–581. <http://doi.org/10.1175/2009jcli2662.1>
- Perlin, N., de Szoeke, S. P., Chelton, D. B., Samelson, R. M., Skillingstad, E. D., & O'Neil, L. W. (2014). Modeling the atmospheric boundary layer wind response to mesoscale sea surface temperature perturbations. *Monthly Weather Review*, 142(11), 4284–4307. <https://doi.org/10.1175/MWR-D-13-00332.1>
- Qiu, B. (2000). Interannual variability of the Kuroshio Extension system and its impact on the wintertime SST field. *Journal of Physical Oceanography*, 30(6), 1486–1502. [https://doi.org/10.1175/1520-0485\(2000\)030<1486:IVOTE>2.0.CO;2](https://doi.org/10.1175/1520-0485(2000)030<1486:IVOTE>2.0.CO;2)
- Qiu, B., & Chen, S. M. (2005). Variability of the Kuroshio Extension jet, recirculation gyre, and mesoscale eddies on decadal time scales. *Journal of Physical Oceanography*, 35(11), 2090–2103. <https://doi.org/10.1175/jpo2807.1>
- Renault, L., Molemaker, M. J., McWilliams, J. C., Shchepetkin, A. F., Lemarie, F., Chelton, D., et al. (2016). Modulation of wind work by oceanic current interaction with the atmosphere. *Journal of Physical Oceanography*, 46(6), 1685–1704. <https://doi.org/10.1175/jpo-d-15-0232.1>
- Seo, H., Miller, A. J., & Norris, J. R. (2016). Eddy-wind interaction in the California Current System: Dynamics and impacts. *Journal of Physical Oceanography*, 46(2), 439–459. <https://doi.org/10.1175/jpo-d-15-0086.1>
- Small, R. J., deSzoeke, S. P., Xie, S. P., O'Neill, L., Seo, H., Song, Q., et al. (2008). Air-sea interaction over ocean fronts and eddies. *Dynamics of Atmospheres and Oceans*, 45(3-4), 274–319. <https://doi.org/10.1016/j.dynatmoce.2008.01.001>
- Su, Z., Wang, J. B., Klein, P., Thompson, A. F., & Menemenlis, D. (2018). Ocean submesoscales as a key component of the global heat budget. *Nature Communications*, 9(1), 775. <https://doi.org/10.1038/s41467-018-02983-w>
- Sugimoto, S., & Hanawa, K. (2005). Remote reemergence areas of winter sea surface temperature anomalies in the North Pacific. *Geophysical Research Letters*, 32(1), L01606. <https://doi.org/10.1029/2004GL021410>
- Thomas, L., & Ferrari, R. (2008). Friction, frontogenesis, and the stratification of the surface mixed layer. *Journal of Physical Oceanography*, 38(11), 2501–2518. <https://doi.org/10.1175/2008JPO3797.1>
- von Storch, J. S., Eden, C., Fast, I., Haak, H., Hernandez-Deckers, D., Maier-Reimer, E., et al. (2012). An estimate of the Lorenz energy cycle for the world ocean based on the 1/10 degrees STORM/NCEP simulation. *Journal of Physical Oceanography*, 42(12), 2185–2205. <https://doi.org/10.1175/jpo-d-12-079.1>
- Xue, H. J., Bane, J. M., & Goodman, L. M. (1995). Modification of the Gulf-Stream through strong air-sea interactions in winter: Observations and numerical simulations. *Journal of Physical Oceanography*, 25(4), 533–557. [https://doi.org/10.1175/1520-0485\(1995\)025<0533:MOGST>2.0.CO;2](https://doi.org/10.1175/1520-0485(1995)025<0533:MOGST>2.0.CO;2)
- Yang, P., Jing, Z., & Wu, L. (2018). An assessment of representation of oceanic mesoscale eddy-atmosphere interaction in the current generation of general circulation models and reanalyses. *Geophysical Research Letters*, 45(21), 11,856–11,865. <https://doi.org/10.1029/2018GL080678>